JOURNAL OF SPACECRAFT AND ROCKETS
Vol. 47, No. 4, July–August 2010

Technical Notes

Shape Optimization for Hypersonic Arc-Wing Missiles

Kai Cui*
Chinese Academy of Sciences, Beijing 100190, China
and
Guo-wei Yang†
Chinese Academy of Sciences, Beijing 100190, China

DOI: 10.2514/1.45882

Nomenclature

A_{att}	=	angle of attack, deg
C_D	=	drag coefficient
C_L	=	lift coefficient
Ma	=	Mach number
P_0	=	total pressure, Pa
P_∞	=	static pressure, Pa
Re	=	Reynolds number, m^{-1}
T_0	=	total temperature, K
x	=	design variables for optimization
θ_a	=	fixing angle in tangential direction of wings, deg
θ_w	=	sweepback angle of wings, deg

Subscripts

com	=	computational
exp	=	experimental
optm	=	optimized
orin	=	original (initial)
trim	=	modified by considering the head shock wave

I. Introduction

OPTIMIZATION has become a powerful tool to greatly enhance the performances of trajectory [1], propulsion [2], and structure [3,4] for various kinds of aircrafts, while considerable efforts have been made for the development of aerodynamic shape optimization of nonaxisymmetric hypersonic airbreathers and their components. A multidisciplinary design optimization process was developed and successfully applied to a hypersonic missile concept by Bowcutt [5], which produced an optimized configuration with a dramatic 46% range increase over a baseline vehicle. Gaiddon et al. [6] carried out mono- and multi-objective optimizations for the supersonic inlet of a ramjet powered missile by applying computational fluid dynamics (CFD) to aerodynamic prediction and theoretical modeling of engine performances. Starkey and Lewis [7] analyzed and optimized a series of hydrocarbon-fueled, hypersonic waverider-based missiles that were constrained to fit within a fixed geometric box, in which a pareto-based evolutionary optimization with exponential apportioning was performed using the shareware code IMPROVE. In addition, there are many other instructive works on waveriders or integrated hypersonic vehicles [8–10].

By contrast, only a few studies on aerodynamic shape optimization have been found in respect of axisymmetric configurations. The work of Anderson et al. [11] was focused on applying genetic algorithms to determine high-efficiency missile geometries with a variety of design goals and constraints given. Hartfield et al. [12] also used a genetic algorithm as the driver of symmetric-center-body ramjet powered missiles' optimization process, and the results benefit greatly the preliminary design of missiles. A step by step updated neural network was adopted by Su et al. [13] as the approximate model in the optimization cycle to reduce computational time, and an analogical strategy of combining radial basis function neural networks with evolutionary algorithms was adopted by Deepak et al. [14] to minimize the drag force of a nose cone used in hypersonic flight experiments.

As given by the Breguet range equations, the lift-to-drag ratio (L/D) of a vehicle is in direct proportion to its cruise range. For an axisymmetric missile configuration powered either by ramjets or by rockets, wings should be sufficiently large to guarantee a high L/D. However, the shape and the area of wings are often spatially limited by the confined launch tube. One of the design tradeoffs of this contradiction is to adopt folding arc-wings as shown in Fig. 1, where the adjustable arc-wings are enwrapped in the body before launch to save space, and expanded after the missile begins to cruise to gain a high aerodynamic performance. Obviously, the arc-wings play a key role for assuring a high L/D for the missile.

In this Note, the leading edge (LE) and the fixing angle in the wing's tangential direction θ_a are optimized for the sake of improving the aerodynamic performance of a generic hypersonic missile. A Nelder–Mead simplex algorithm [15] is used as the driver of the optimization cycle, and the aerodynamic coefficients are evaluated by CFD analysis. Furthermore, both a fast Euler equation solver and an accurate Navier–Stokes equation solver are alternately employed

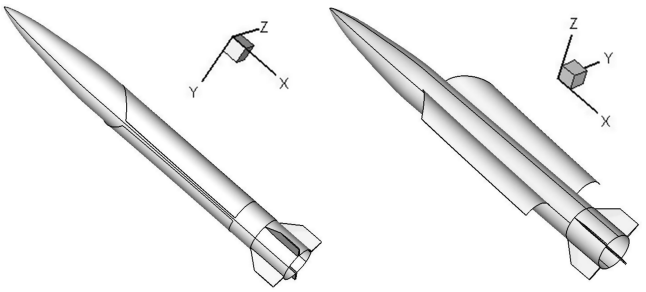

Fig. 1 Folding (left) and unfolding (right) status of an arc-wing missile.

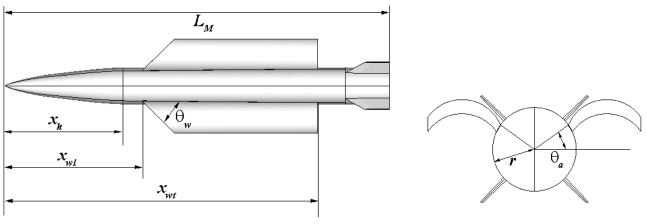

Fig. 2 Top (left) and rear (right) views of the baseline model.

Received 8 June 2009; revision received 8 January 2010; accepted for publication 23 February 2010.

*Associate Professor, Key Laboratory of High Temperature Gas Dynamics, Institute of Mechanics, Chinese Academy of Sciences, Number 15, Beisihuanxi Road; kcui@imech.ac.cn. State Key Laboratory of Structural Analysis for Industrial Equipment, Dalian University of Technology.

†Professor, Key Laboratory of High Temperature Gas Dynamics, Institute of Mechanics, Chinese Academy of Sciences, Number 15, Beisihuanxi Road; gwyang@imech.ac.cn.

Table 1 Dimensionless value of the baseline model

L_M	x_{wl}	x_{wt}	x_h	r
1	0.3568	0.814	0.3122	0.0483

to suit different conditions and to balance costs and accuracy of the computation.

II. Geometrical Model and Parameterization

The top and the rear views for the baseline are shown in Fig. 2, with dimensionless values of key geometrical parameters listed in Table 1. The assemble angle between the wings and the body is fixed at 1 deg, and θ_a and θ_w are 30 and 45 deg, respectively.

For this configuration, the projection of the LE on the base plane is a circular arc with radius r to assure the folding wings wrapping the body, and thus the spatial LE can be uniquely defined by its two-dimensional projection on the top view. A cubic B-spline function [16,17] is adopted to parameterize the two-dimensional LE.

The shape of LE is uniquely determined by four independent control points, as illustrated in Fig. 3. Here point 1 is the fixed joint between the wing and the body, and Y coordinate of point 4 is constrained by the wingspan, which is also a fixed value. Moreover, a primary study finds that the Y coordinates of point 2 and 3 are not sensitive to the aerodynamic force of the missile, and thus only three variables, the X coordinates of point 2, 3, and 4, are selected as the design variables for optimizing the LE of wings.

III. Aerodynamic Evaluation Tool and Validation

Aerodynamic governing equations are the steady, three-dimensional thin layer Navier–Stokes equations in the conservation form. The effect of gas dissociation is not considered because the missile works in the low hypersonic regime of Mach 6. In addition, because the validation data for CFD are obtained from a geometrically scaled wind tunnel experiment (the total length is about 0.6 m), the turbulence effect can be neglected to a certain extent. The inviscid terms of the governing equations are approximated by the standard upwind-based flux-difference-splitting scheme of Roe [18]; the viscous terms are discretized by the second-order central difference. The unstructured tetrahedral grid is used, and the triangle meshes on the missile surface are refined to capture the boundary layer (the gird density of the surface is about 0.8E-3 mm for the validation model). Flow conditions for both the wind tunnel experiments and the computation are identical, as shown in Table 2, and the experimental results are listed in Table 3.

The comparisons of aerodynamic coefficients between computational and experimental results are given in Fig. 4, which clearly shows that the numerical results fit the wind tunnel data very well, with maximal error less than 5%. The size of computational field and the grid dimension of the above examples are then extended to all the computational cases covered in this paper to assure the computational accuracy. As shown in Fig. 4, the peak value of L/D appears at 6 deg angle of attack on the basis of numerical and experimental results, and thus the flow conditions listed in Table 2 and the 6 deg angle of attack are accordingly taken as the design point in the following analyses.

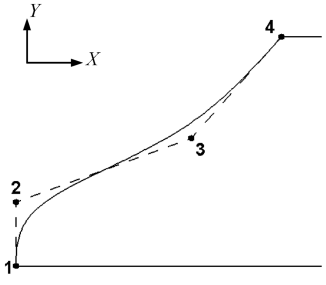

Fig. 3 Example of the LE parameterization.

Table 2 Flowfields conditions of the wind tunnel experiments

Ma	P_0	P_∞	T_0	Re
6	2,061,065	1398.547	464.4456	2.06359E7

Table 3 Wind tunnel experiment results

A_{att}	C_L	C_D	L/D
0	0.2881	0.1724	1.6714
4	1.0663	0.2716	3.9261
6	1.5201	0.3747	4.0565
8	1.9901	0.5163	3.8545

IV. Optimization

A. Sweepback Optimization

The flowchart of the optimization cycle is shown in Fig. 5. A series of heuristic computations for configurations with different θ_w are performed, and their configurations and L/D at the design point are shown in Fig. 6. According to this figure, the maximal value of L/D appears at $\theta_w = 0$, and thus the variation of design variables should be confined to $x < x_{wl}$.

B. Optimization of the Fixing Angle in Tangential Direction θ_a

The optimal θ_a is also determined by several heuristic computations, and the lower and the upper bounds of θ_a are -15 and $+30$ deg, respectively. The peak value of L/D is searched out at $\theta_a = 11$ deg after six trial evaluations. The two-dimensional and three-dimensional views of all trial configurations are shown in Fig. 7, and the values of L/D in all the trial configurations are shown in Fig. 8.

The reason why there exists an optimal θ_a might be explained as follows. To begin with, the arc-wings are the main components for generating lift as discussed above, and the wings with large area generally lead to high lift and high drag simultaneously. Because the arc-wings should wrap the body without any overlap in folding status, the arc length as well as the area of wings is mainly determined by θ_a. Next, because the missile compresses the freestream when it flies at its design point, a high pressure zone is naturally generated and exists mainly beneath the head part, as shown in Fig. 9. Furthermore, the high pressure wears off along the longitudinal direction and diminishes from bottom to top in each transversal profile of the missile. When the high pressure acts on the arc-wings, the missile acquires an additional lift, and thus the distance between the wings and the bottom of the missile (the position of the highest pressure zone), which is uniquely determined by and directly proportional to the value of θ_a, will remarkably impact on the L/D of the missile. The lower the value of θ_a, the shorter the distance between the wings and the bottom of the missile, and the higher the pressure on the low surface of the wings. On the other hand, the lower value of θ_a also leads to smaller area of wings. The above discussion shows that the wingspan of the missile should be carefully selected to assure adequate wing area and to capture the high pressure as much as possible, resulting in an optimal θ_a.

C. Shape Optimization of LE of Wings

The LE of wings (described by three variables) is optimized numerically to maximize the L/D of the missile. Based on the above results, the optimization problem can be formulated as follows:

$$\min -L(\tilde{x})/D(\tilde{x}) \tag{1}$$

$$s.t. \quad x_i \le x_{wl} \qquad x_i \ge x_h \ (i = 1, \ldots, 3) \tag{2}$$

where x_h represents the joint position between the missile head and the body. The nonlinear simplex method of Nelder and Mead is used as the optimizer.

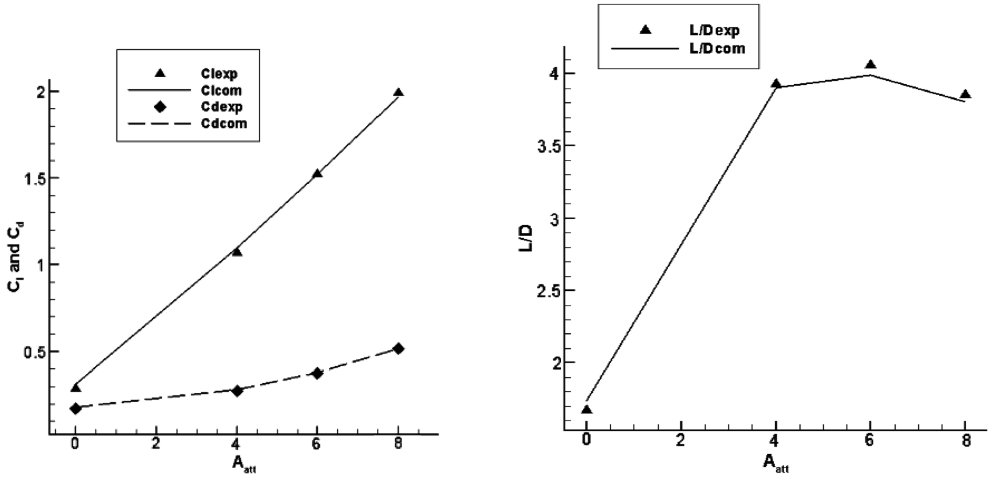

Fig. 4 Lift and drag coefficient (left) and L/D (right) comparison between the computational and the experimental results.

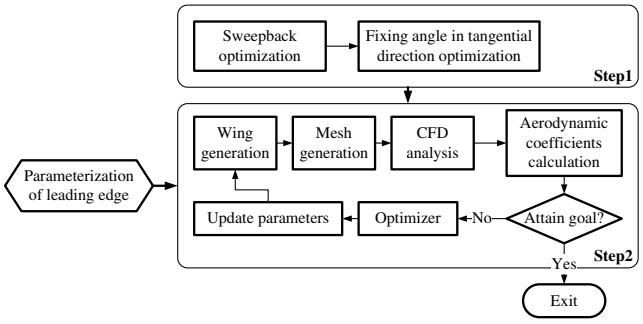

Fig. 5 Flowchart of the optimization.

Two simplification techniques are adopted in order to save computational efforts. First, the unique variable part is the wing in the LE optimization cycle, while the part behind the wings (the tail) remains unchanged during the optimization. It is well-known that a disturbance will not spread upstream in hypersonic regime, and thus a curtailed configuration, as shown in Fig. 10, can be used in the optimization iteration without influencing the correctness of results. This leads to a decrease of grid number. Next, although the area of wings changes continually in the optimization iteration, the variation of the changing part occupies a small portion of the whole missile area. Obviously, the variation of the surface friction related mainly to the missile area can be neglected during the optimization. Therefore, it is feasible that the time-consuming Navier–Stokes equations

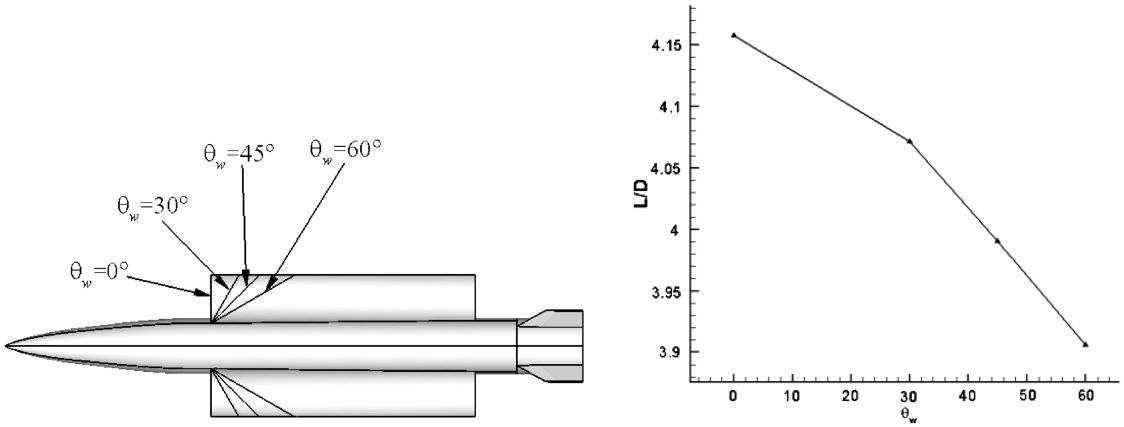

Fig. 6 Configurations (left) and their L/D (right) with different sweepback angle.

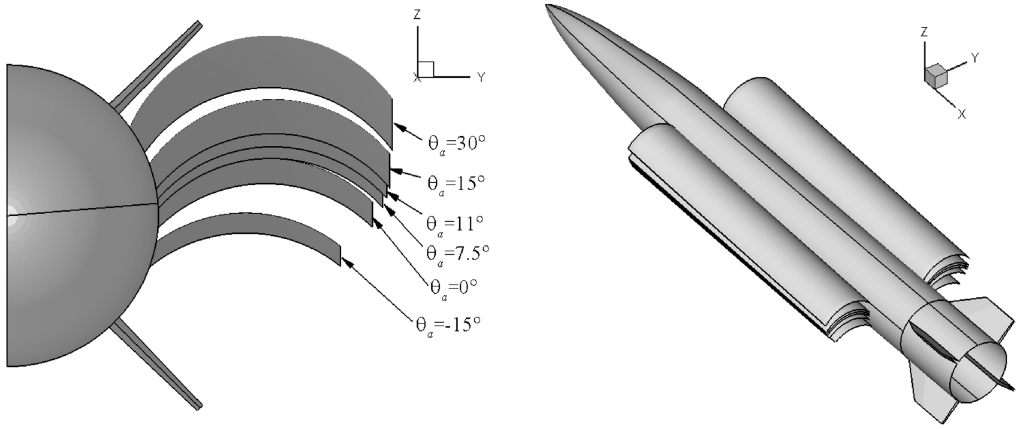

Fig. 7 Two-dimensional and three-dimensional views of the trial configurations with θ_a variation.

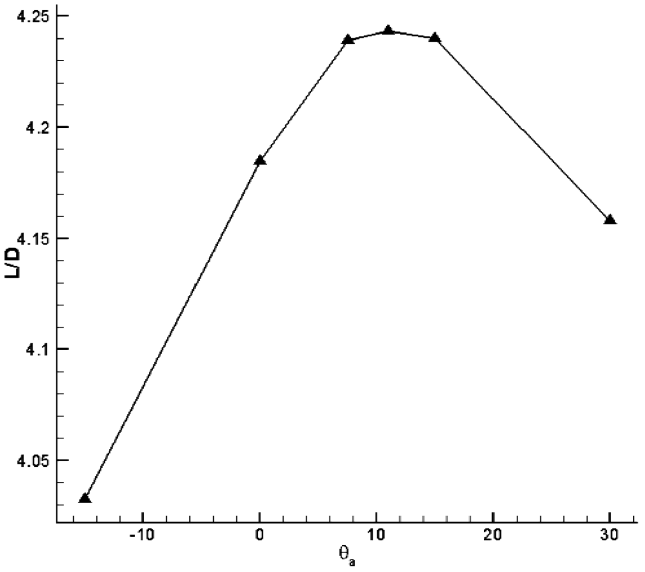

Fig. 8 L/D of the trial configurations vs θ_a.

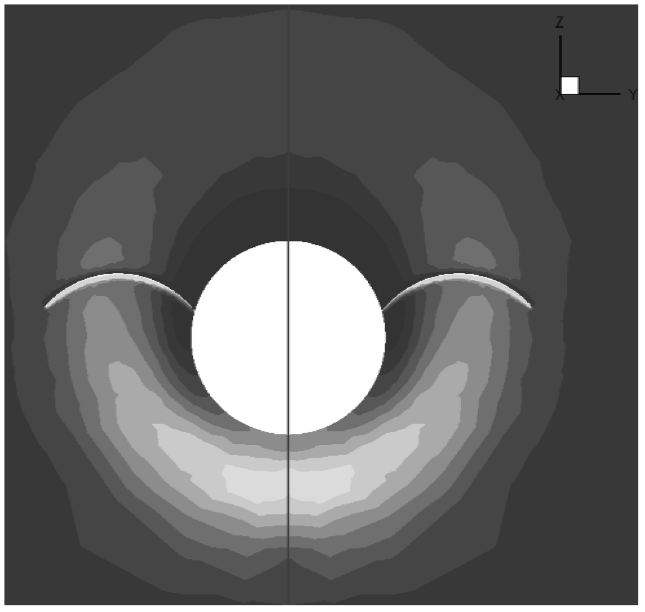

Fig. 9 Example of the high pressure zone beneath the missile.

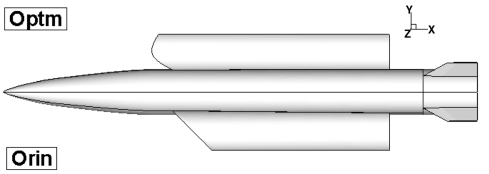

Fig. 11 Comparison between the initial and the optimal wings.

solver is replaced by a time-saving Euler equations solver in the optimization loop. By applying these two techniques, more than 70% computational costs can be saved.

The comparison between the initial and the optimal wing shape is shown in Fig. 11. The aerodynamic coefficients calculated by the Navier–Stokes equations solver and the increments of coefficients are shown in Tables 4 and 5, respectively.

According to Tables 4 and 5, the lift coefficient increases after the optimization, while the drag coefficient reduces at the design point. The amelioration of lift and drag leads directly to the L/D gains, an 8.76% improvement. In addition, the values of L/D also increase around the design point (at 4 and 8 deg angle of attack). Along the axial direction of missile, the pressure contours in the initial and the optimized cases are shown in Fig. 12.

From Figs. 11 and 12, it is evident that the sweepback wings transform to sweepforward after the optimization. Therefore, the high pressure generated by the head can be much better captured by the sweepforward wings, which is the main reason for the gain of the axial force and the lift. In addition, the reduction of wingspan that profits from the variation of fixing angle in the tangential direction leads to a palpable drop of drag. As a result, the L/D acquires a considerable increment.

D. Modification of Wings by Considering the Head Shock

By contrast with the original sweepback wings, the optimized wings are sweepforward. However, if the shock wave that derived from the missile head intersects the wings, the missile may be destroyed, and thus it is very important to determine the position of the head shock. The inviscid flowfield around the missile head is calculated by solving the Euler equations numerically, in which a structured grid with H-type topology is used to discretize the computational domain, as shown in Fig. 13. Moreover, a solution-based adaptive grid is employed to achieve a good shock resolution; i.e., the regions with high pressure gradient are captured as the shock layer, where the grids are allowed to recluster. The result of Fig. 14 reveals that the head shock does intersect the sweepforward wings.

Intuitively, the segment of wings outside the head shock has to be trimmed to avoid this danger, as shown in Fig. 15. The aerodynamic parameters of the missile with trimmed wings are shown in Table 6.

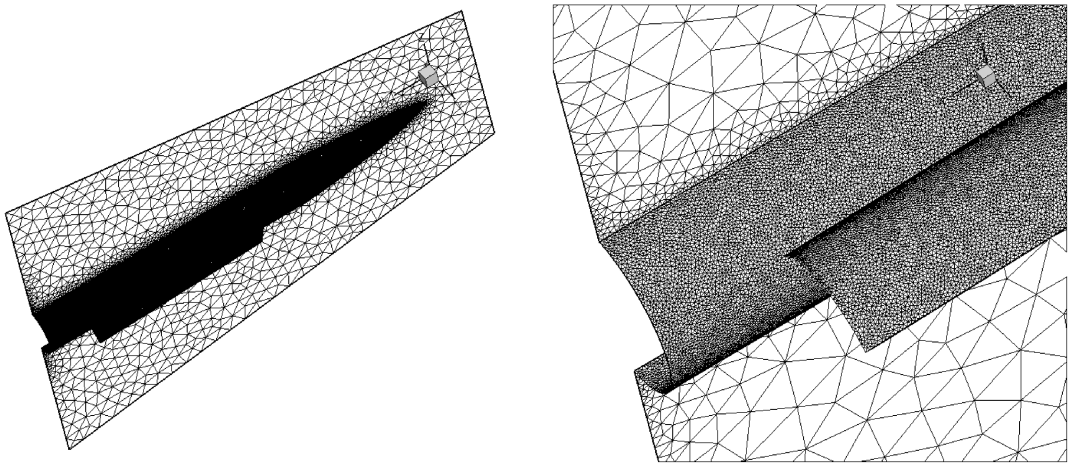

Fig. 10 Full (left) and local (right) zone of the curtailed configurations.

Table 4 Aerodynamic coefficients of the optimized missile

A_{att}	C_L	C_D	L/D
0	0.1938	0.1663	1.1658
4	1.0745	0.2578	4.1676
6	1.5606	0.3596	4.3400
8	2.0373	0.5044	4.1379

Table 5 Increments of aerodynamic coefficients after the optimization

A_{att}	ΔC_L	ΔC_D	$\Delta(L/D)$
0	−38.24%	−7.79%	−33.02%
4	−2.08%	−8.34%	6.83%
6	2.69%	−5.58%	8.76%
8	3.47%	−2.52%	8.76%

By comparing the results of Tables 4 and 6, it is clear that the differences of the L/D between the optimized and the trimmed wings are relatively small.

The relative variation of the important aerodynamic and geometrical parameters of the optimized and the trimmed configurations in comparison with the initial one are shown in Table 7, from which it is clear that the drag of the trimmed configuration is lower than the optimized one, while the L/D of the former is higher than the latter. In comparison with the initial wings, the area and the wingspan of the trimmed wings are diminished by 1.7 and 7.66%, respectively. The reduction of wings area lightens the weight of missile, while the reduction of wingspan will benefit the wing's structural strength.

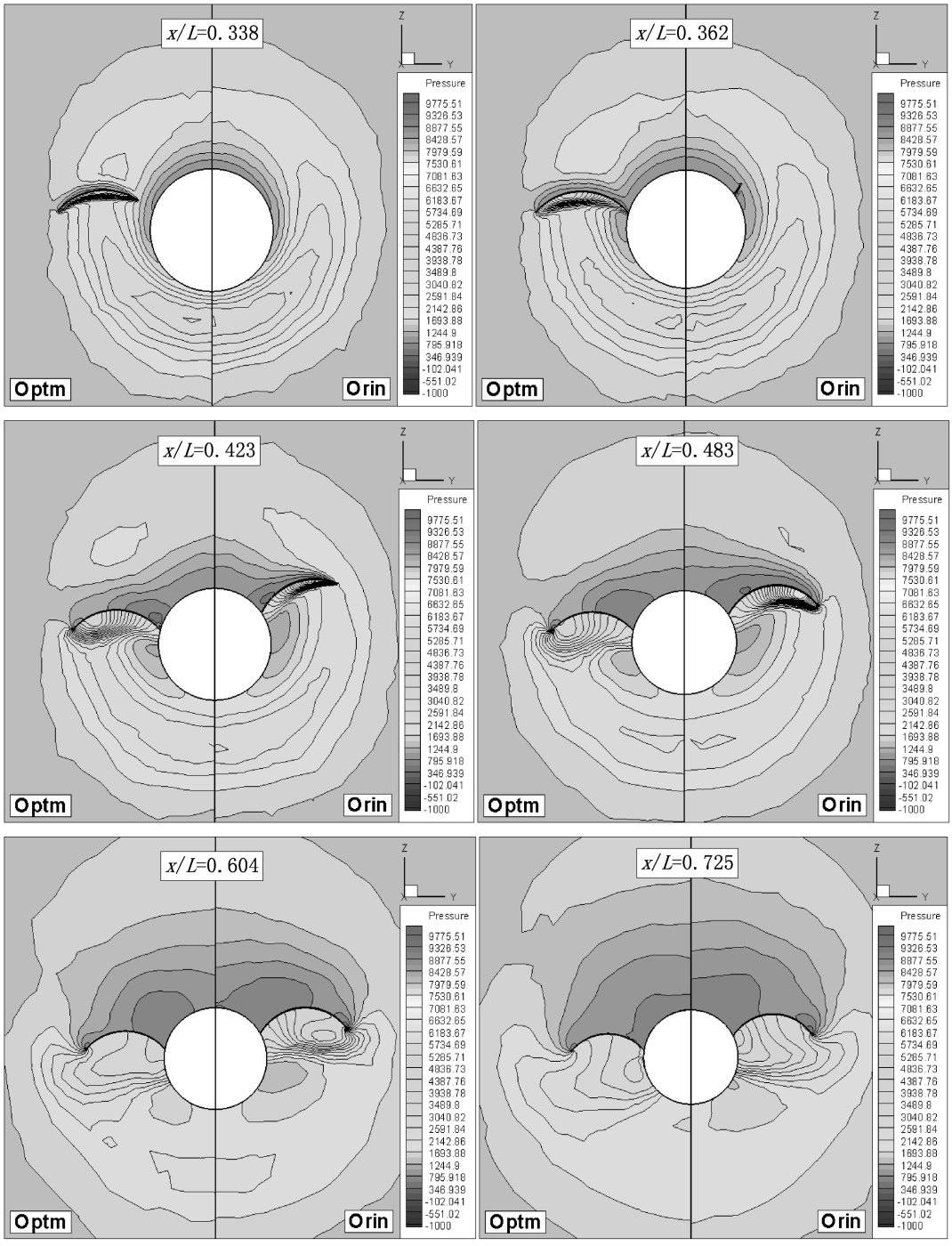

Fig. 12 Pressure contours comparison between the initial and the optimized configurations at the design point.

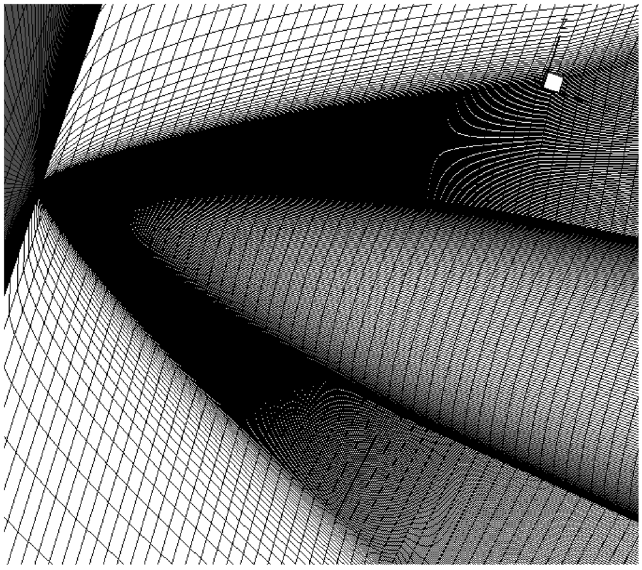

Fig. 13 Structured grids for capture nose shock.

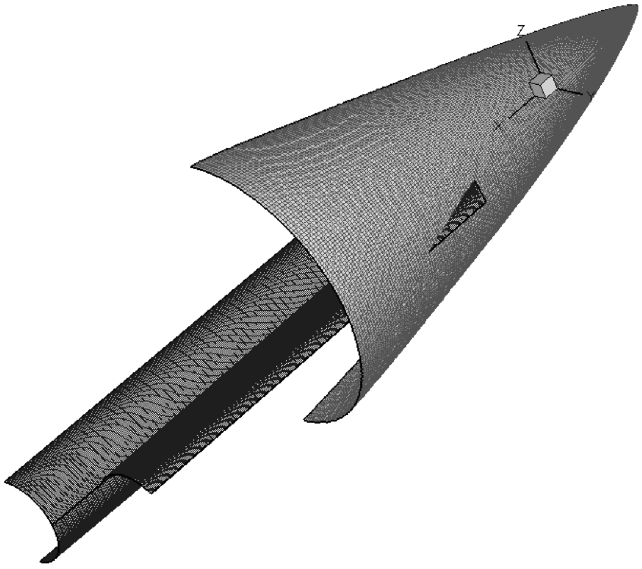

Fig. 14 Captured nose shock.

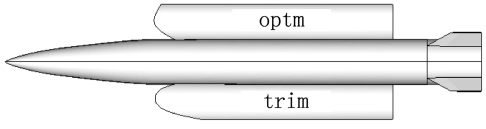

Fig. 15 Comparison between the optimized and the trimmed wing.

Table 6 Aerodynamic coefficients for the trimmed-wing missile

A_{att}	C_L	C_D	L/D
0	0.1841	0.1596	1.1540
4	1.0502	0.2500	4.2011
6	1.5241	0.3497	4.3585
8	2.0327	0.4767	4.1381

Table 7 Increments of the key aerodynamic and geometrical parameters

	ΔC_L	ΔC_D	$\Delta L/D$	ΔA	ΔW
Optm	+2.69 %	−5.58 %	+8.76 %	+1.5 %	−7.66 %
Trim	+0.2 %	−8.18 %	+9.22 %	−1.7 %	−7.66 %

V. Conclusions

An optimization study was conducted to generate a hypersonic missile shape with higher aerodynamic performance compared with the original configuration. Both the fixing angle in tangential direction and the lead edge shape of the folding arc-wings are optimized by adopting the Nelder–Mead simplex method. The aerodynamic coefficients are evaluated by an inviscid flowfield solver in the optimization cycle for reducing computational costs, while an accurate Navier–Stokes equations solver is used to calculate the aerodynamic performance of the baseline, the optimized, and the trimmed configurations for assuring computational accuracy. In addition, a curtailed configuration is involved in the optimization for further saving computer time. Furthermore, the shape of wings is trimmed to ensure the safety of the missile based on analyzing the head shock's influences. In addition, the wing area of the trimmed configuration is also smaller than the optimized one. Therefore, the hypersonic missile configuration with trimmed wings is preferable.

On the basis of the present results, we can draw the following conclusions, which can also be directly applied to other aerodynamic optimization problems for various kinds of supersonic or hypersonic vehicles. First, the strategy of incorporating the Nelder–Mead simplex method with CFD analysis can be applied to the optimization of hypersonic missiles and can improve the comprehensive performance of missiles. Next, an appropriate sweepforward wing design may efficiently ameliorate the aerodynamic performance by dint of the high pressure generated by the missile head, especially in the hypersonic regime. In addition, an accurate tool, such as a CFD solver, may be indispensable for correctly reflecting the coupling effect between missile body and wings because it plays an important role in elevating the L/D of missile at the design point [19]. Last but not least, combination of the accurate Navier–Stokes solver and the fast Euler solver can effectively reduce the computational costs without influencing the optimization results.

Acknowledgments

This research was supported by the National Natural Science Foundation of China (Grant No. 90916013) and the State Key Laboratory of Structural Analysis for Industrial Equipment, Dalian University of Technology.

References

[1] Li, Y., Cui, N. G., and Rong, S. Y., "Trajectory Optimization for Hypersonic Boost-Glide Missile Considering Aeroheating," *Aircraft Engineering and Aerospace Technology*, Vol. 81, No. 1, 2009, pp. 3–13. doi:10.1108/00022660910926854

[2] Riddle, D. B., Hartfield, R. J., Burkhalter, J. E., and Jenkins, R. M., "Genetic-Algorithm Optimization of Liquid-Propellant Missile Systems," *Journal of Spacecraft and Rockets*, Vol. 46, No. 1, 2009, pp. 151–159. doi:10.2514/1.30891

[3] Luo, Z., Yang, J. Z., and Chen, L. P., "A New Procedure for Aerodynamic Missile Designs Using Topological Optimization Approach of Continuum Structures," *Aerospace Science and Technology*, Vol. 10, No. 5, 2006, pp. 364–373. doi:10.1016/j.ast.2005.12.006

[4] Jun, S., Tischler, V. A., and Venkayya, V. B., "Multidisciplinary Design Optimization of a Built-Up Wing Structure with Tip Missile," *Journal of Aircraft*, Vol. 40, No. 6, 2003, pp. 1093–1098. doi:10.2514/2.7219

[5] Bowcutt, K. G., "Multidisciplinary Optimization of Airbreathing Hypersonic Vehicles," *Journal of Propulsion and Power*, Vol. 17, No. 6, 2001, pp. 1184–1190. doi:10.2514/2.5893

[6] Gaiddon, A., Knight, D. D., and Poloni, C., "Multicriteria Design Optimization of a Supersonic Inlet Based Upon Global Missile Performance," *Journal of Propulsion and Power*, Vol. 20, No. 3, 2004, pp. 542–558. doi:10.2514/1.2390

[7] Starkey, R. P., and Lewis, M. J., "Critical Design Issues for Airbreathing Hypersonic Waverider Missiles," *Journal of Spacecraft and Rockets*, Vol. 38, No. 4, 2001, pp. 510–519. doi:10.2514/2.3734

[8] Starkey, R. P., Rankins, F., and Pines, D., "Coupled Waverider/ Trajectory Optimization for Hypersonic Cruise," AIAA Paper 2005-530, 2005.
[9] Lobbia, M., and Suzukit, K., "Design and Analysis of Payload-Optimized Waveriders," AIAA Paper 2001-1849, 2001.
[10] Takashima, N., and Lewis, M. J., "Optimization of Waverider-Based Hypersonic Cruise Vehicles with Off-Design Considerations," *Journal of Aircraft*, Vol. 36, No. 1, 1999, pp. 235–245. doi:10.2514/2.2430
[11] Anderson, M. B., Burkhalter, J. E., and Jenkins, R. M., "Missile Aerodynamic Shape Optimization Using Genetic Algorithms," *Journal of Spacecraft and Rockets*, Vol. 37, No. 5, 2000, pp. 663–669. doi:10.2514/2.3615
[12] Hartfield, R. J., Jenkins, R. M., and Burkhalter, J. E., "Ramjet Powered Missile Design Using a Genetic Algorithm," *Journal of Computing and Information Science in Engineering*, Vol. 7, No. 2, 2007, pp. 167–173. doi:10.1115/1.2738722
[13] Su, W., Zuo, Y., and Gao, Z., "Preliminary Aerodynamic Shape Optimization Using Genetic Algorithm and Neural Network," AIAA Paper 2006-7106, 2006.
[14] Deepak, N. R., Ray, T., and Boyce, R. R., "Evolutionary Algorithm Shape Optimization of a Hypersonic Flight Experiment Nose Cone," *Journal of Spacecraft and Rockets*, Vol. 45, No. 3, 2008, pp. 428–437. doi:10.2514/1.33826
[15] Nelder, J. A., and Mead, R., "A Simplex Method for Function Minimization," *Computer Journal*, Vol. 7, No. 4, 1965, pp. 308–313.
[16] Cui, K., Zhao, D. X., and Yang, G. W., "Waverider Configurations Derived from General Conical Flowfields," *Acta Mechanica Sinica*, Vol. 23, No. 3, 2007, pp. 247–255. doi:10.1007/s10409-007-0069-2
[17] Cui, K., and Yang, G. Wei., "The Effect of Conical Flowfields on the Performance of Waveriders at Mach 6," *Chinese Science Bulletin*, Vol. 52, No. 1, 2007, pp. 57–64.
[18] Roe, P. L., "Characteristic Based Schemes for the Euler Equations," *Annual Review of Fluid Mechanics*, Vol. 18, 1986, pp. 337–365. doi:10.1146/annurev.fl.18.010186.002005
[19] Tsuchiya, T., and Takenaka, Y., "Multidisciplinary Design Optimization for Hypersonic Experimental Vehicle," *AIAA Journal*, Vol. 45, No. 7, 2007, pp. 1655–1662. doi:10.2514/1.26668